

## OS2-6

## 微小重力環境下における Fe-Cu 合金の相分離

Phase separation of Fe-Cu alloys under microgravity  
condition

正木匡彦<sup>1</sup>, 敷地駿<sup>1</sup>, 望月遥矢<sup>1</sup>, 小嶋秀和<sup>2</sup>, 白鳥英<sup>3</sup>, 小澤俊平<sup>3</sup>, 小山千尋<sup>4</sup>, 石川毅彦<sup>4</sup>, 永山勝久<sup>1</sup>  
Tadahiko Masaki<sup>1</sup>, Shun Shikichi<sup>1</sup>, Haruya Mochizuki<sup>1</sup>, Hidekazu Kobatake<sup>2</sup>, Suguru Shiratori<sup>3</sup>, Shumpei Ozawa<sup>4</sup>,  
Chihiro Koyama<sup>5</sup>, Takehiko Ishikawa<sup>5</sup>, Katsuhisa Nagayama<sup>1</sup>

<sup>1</sup> 芝浦工業大学, Shibaura Institute of Technology,

<sup>2</sup> 同志社大学, Doshisha University,

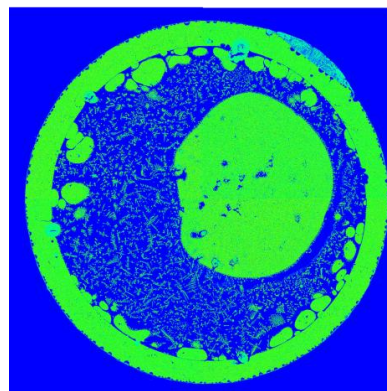
<sup>3</sup> 東京都市大学, Tokyo City University

<sup>4</sup> 千葉工業大学, Chiba Institute of Technology

<sup>5</sup> 宇宙航空研究開発機構, Japan Aerospace Exploration Agency

\* Correspondence: t\_masaki@sic.shibaura-it.ac.jp

**Abstract:** Fe-Cu alloys undergo liquid-liquid phase separation during solidification from a supercooled state, producing core-shell spheres with Fe-rich and Cu-rich phases. Using containerless processing methods such as atomization and gas jet levitation, double or higher core-shell structures have been observed, though their formation mechanisms remain unclear. To investigate, melting/solidification experiments were performed in an electrostatic levitation furnace (ELF) aboard the ISS for Fe-Cu alloys of 30–70 at% Cu in 10% increments. Samples (~2 mm) were prepared in an argon glove box ( $O_2 \leq 100$  ppm), levitated, laser-melted, and naturally solidified in pure argon. Cooling curves were recorded, using the Cu-phase solidification temperature (1369 K) for emissivity correction. EPMA mapping of sectioned samples revealed triple shells with Fe-rich outer/inner layers and a Cu-rich middle layer. The inner shell showed distortion, indicating disturbance during solidification, and Fe-rich domains migrated toward the outer shell. Dendritic Fe phases appeared in Cu-rich layers, and high-oxygen iron oxide domains formed on the outer shell. Results suggest that surface tension differences, strongly influenced by oxygen concentration, and parent-phase volume fraction control phase arrangement. Comparisons of cooling curves and microstructures for all compositions are presented, alongside ground-based results.



**Keywords:** Core shell structure, ELF, Phase separation, Solidification

## 1. Introduction

Fe-Cu alloys exhibit liquid-liquid phase separation during solidification from a supercooled liquid state. By melting and solidifying Fe-Cu alloys without a container using atomization with a short drop tube or a gas jet suspension method, multiple alloy spheres (core-shell structures) composed of a Fe-rich phase (Fe phase) and a Cu-rich phase (Cu phase) are formed. The formation process of these core-shell structures is being elucidated through computer simulations<sup>1</sup>). During the initial phase separation, small droplets form, and due to Marangoni convection caused by temperature differences between the center and surface of sphere, these droplets aggregate and coalesce at the center of the spherical sample, ultimately forming multiple alloy

spheres. At this stage, whether the Fe phase or Cu phase forms the outer shell (shell) or inner shell (core) is influenced by the composition of the homogeneous parent phase and the surface tension difference between the phases after separation. Additionally, while triple or higher core-shell structures have been experimentally obtained, the formation process remains largely unclear.

We successfully observed the formation process of core-shell structures by performing melting and solidification of the Fe-Cu alloy using an electrostatic levitation furnace installed on the International Space Station<sup>2)</sup>. We conducted five experiments with compositions ranging from Fe-30atomic%Cu to Fe-70atomic%Cu in 10atomic% increments and obtained triple core-shell alloy spheres at Fe-50atomic%Cu. Analysis of the solidification microstructures of all five compositions has been completed, and the three-dimensional solidification microstructure has been clarified. In this presentation, we will discuss the relationship between these analysis results and cooling curves, including results from ground-based experiments.

## 2. Experiments and Results of ELF

The spherical samples (diameter 2 mm) used in the ISS experiment were prepared using a gas jet levitation device in an argon-filled glove box. The oxygen concentration in the glove box was maintained at 100 ppm or less. The sample compositions were the five compositions mentioned above, and two to three samples were used for each composition. In the ELF experiment, a sample levitated by electrostatic force were melted by controlling the output of a heating laser, and then the laser output was set to zero to allow natural solidification. The ELF sample atmosphere used pure argon gas, which is the standard gas on the ISS, and pure Zr spheres were heated to remove oxygen from the atmosphere before experiments. The sample temperature was measured using a monochromatic radiometer, and the solidification temperature of the Cu phase (1369 K) was used as the reference temperature for emissivity correction. For samples returned to Earth, surface observations were performed, followed by embedding in resin and grinding every 50 micro meter at a time from the surface. The solidification microstructure and composition distribution were investigated using EPMA mapping. When the area of the sample's analysis surface exceeded the scanning range of the EPMA, multiple analyses were performed by changing the sample position, and the obtained mapping images were combined to clarify the overall solidification structure. Figure 1 shows the cooling curve of Fe-50atomic%Cu after temperature correction. At the point indicated by the arrow in the figure (1565 seconds), the laser output was set to zero.

From the start of cooling until 1568 seconds, the sample position fluctuated and moved out of the detection range of the radiation thermometer, so the approximate cooling curve (guide for eyes) during this period is shown as a dashed line. Similar to the Fe-60atomic% reported last year, multiple releases of solidification latent heat of the Fe phase were observed between 1569 and 1571 seconds.

The solidification structure (EPMA mapping) of the polished surface of the spherical Fe-50atomic% sample is shown in Figure 2. The solidification structure consists of a triple core-shell structure, with the outermost and innermost shells being Fe phase and the layer between them being Cu phase. The innermost shell is not

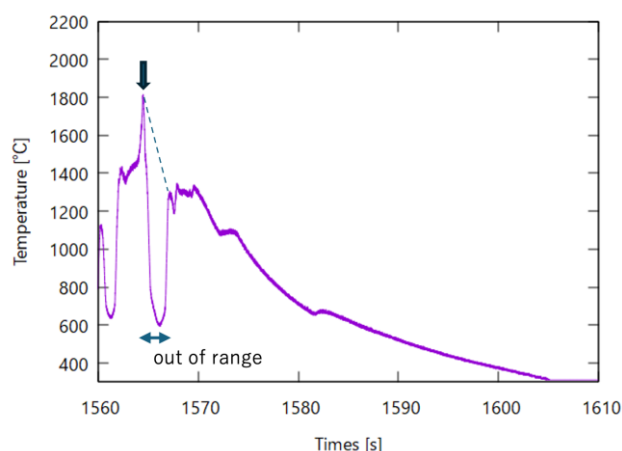


Figure 1 Cooling curve of Fe-50atomic%Cu

The sample was out of range of pyrometer at the time between 1465 and 1568 second. The laser was cut at the time which is indicate an arrow. the sample temperature was normal cooling, the dashline was guide for eyes.

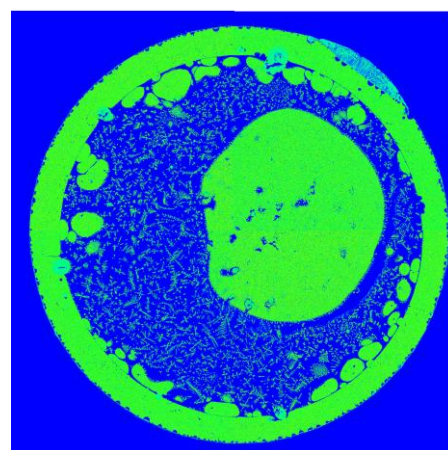


Figure 2 Mappin image of Fe-50atomic%Cu  
The concentration of Fe was indicated by green dots.

completely spherical but distorted, suggesting that it was disturbed during solidification. Multiple small Fe phase domains and domains merging with the outermost shell were observed inside the outermost shell, suggesting that the Fe phase was migrating toward the outermost shell. Numerous Fe phase dendrites were observed in the Cu phase. Additionally, similar to the Fe-60atomic%Cu sample reported last year, domains with high oxygen concentrations (iron oxide domains) were observed outside the outermost shell. Since the surface tension of molten iron strongly depends on the oxygen concentration in the atmosphere, it has become clear that the surface tension of the liquid phase and the volume fraction of the parent phase are involved in the phase arrangement of the core-shell in conditions with high atmospheric oxygen concentrations, such as those in this experiment. In the presentation, we will discuss the relationship between cooling curves of other compositions and solidification phases.

## References

- 1) Y.H. Wu, W.L. Wang, J. Chang, B. Wei, J. Alloys and Compounds 808-814, 763(2018).
- 2) T. Ishikawa, C. Koyama, H. Oda, H. Saruwatari, P.-F. Paradis, Int. J. Microgravity Sci. Appl. 390101, 39 (2022).



© 2025 by the authors. Submitted for possible open access publication under the terms and conditions of the Creative Commons Attribution (CC BY) license (<http://creativecommons.org/licenses/by/4.0/>).